



OPEN Spatiotemporal changes in habitat quality and driving factors in South Hunan mining urban agglomerations, China

Yiming Song^{1,2,6}, Xin Li^{3,6}, Yanlin Yin², Chao Zhao¹, Hongzhou Wang⁴, Ziqi Cai⁵, Zhe Dai² & Yonghong Liu²✉

The development of urban agglomerations driven by the mining industry inevitably impacts regional habitat quality. Understanding how habitat quality evolves over time and space, as well as identifying the key driving factors in mining urban agglomerations, is essential for developing sustainable policies and maintaining ecological security. This study evaluates the spatiotemporal changes in habitat quality from 1990 to 2020 via the InVEST model, forecasts habitat quality in 2040 under various development scenarios via the PLUS model, and investigates the factors contributing to these changes. The results revealed that from 1990 to 2020, areas of forestland, cultivated land, and grassland initially increased before declining, whereas areas of construction land and water bodies continuously expanded, with construction land primarily replacing cultivated land and forestland. The average habitat quality ranged from 0.72 to 0.82 during this period, showing an overall increase followed by a decline, with lower habitat quality found in the central areas and higher quality in the surrounding regions. Additionally, habitat quality exhibited significant spatial autocorrelation, with a slow expansion of low-habitat-quality clusters. Under all three development scenarios for 2040, the region is expected to remain dominated by cultivated land and forest, but with a notable expansion of built-up areas compared with that in 2020. Habitat quality is predicted to decrease by 2040, with an increase in worst-grade areas. On the basis of random forest and geodetector analyses, the main drivers of habitat quality are elevation, slope, and population density, with the most significant interactions occurring between population density and elevation, followed by interactions between nighttime light intensity and elevation and between population density and slope. These results suggest that habitat quality in the region is influenced primarily by the interplay of topography, human development, and economic activities. This study provides valuable insights for the construction of an ecological security framework for mining urban agglomerations.

Keywords Habitat quality, Trend analysis, Future scenario modeling, Key drivers, Mining urban agglomerations

The global surge in resource extraction has intensified ecological changes in mining regions, prompting widespread scholarly focus on habitat quality (HQ)¹. The mining sector, while pivotal for economic advancement, has concurrently caused profound ecological challenges². Studies indicate that mining-centric urban clusters exhibit distinctive aggregation effects, where the intensive extraction of minerals leads to an expansion of associated industrial and residential land, consequently diminishing agricultural land, reducing wildlife habitats, and posing threats to biodiversity³. Globally, mining centers such as the Amazon Basin and the Witwatersrand Basin are already experiencing similar problems, where uncontrolled exploitation has led to irreversible ecological damage^{4,5}. In light of increasing ecological conservation awareness, global attention to HQ has intensified. This focus is driven by the understanding that HQ not only is critical for species survival and reproduction but also directly influences human health and quality of life⁶. Consequently, examining the changes in HQ within

¹Academy of Arts and Design, Tsinghua University, Beijing 100084, China. ²School of Design, Hunan University, Changsha 410082, China. ³College of Forestry, Beijing Forestry University, Beijing 100083, China. ⁴School of National Safety and Emergency Management, Beijing Normal University, Beijing 100875, China. ⁵Student Mental Health Education Center, Hunan University of Technology and Business, Changsha 410205, China. ⁶Yiming Song and Xin Li contributed equally to this work. ✉email: liuyh@hnu.edu.cn

mining cities, understanding their spatial and temporal dynamics, and identifying their underlying drivers are essential. Such research can inform the creation of evidence-based strategies for sustainable development, thereby bolstering biodiversity conservation, ecological balance, and stability in these regions.

HQ indicates a region's capacity to offer appropriate living conditions for species and populations⁷. High-quality habitats can increase ecological stability and resilience to external disturbances^{8,9}. Current methods for assessing HQ at the regional scale involve primarily field surveys and ecological assessment models¹⁰. Field surveys are mainly applicable to small-scale regional assessments¹¹ but they are time-consuming and labor-intensive, and obtaining long-term species data poses a significant challenge¹² often making it difficult to evaluate the spatiotemporal dynamics of ecological functions such as biodiversity¹³. In order to overcome these limitations, ecological assessment models that utilize multi-source remote sensing data for spatial and visual representation of HQ have emerged as powerful tools to characterize spatial and temporal variations in HQ in a vivid way^{14,15}. These models include SolVES, HSI, and InVEST, among others^{16–18}. Notably, the InVEST model boasts advantages such as ease of data acquisition, high accuracy, and strong spatial expression capabilities¹⁹ enabling the reflection of habitat distributions and degradation patterns in different landscape types, and thus has garnered widespread attention²⁰. Unfortunately, the application of the model in HQ assessments of mining urban agglomerations where mining development, rapid urbanization and fragile ecosystems coexist is still limited.

Mine HQ is influenced by a combination of economic, social, and natural geographic factors at various scales²¹. Economic and social factors include land use, population density, gross domestic product (GDP), industrial activities, and commercial operations, whereas natural geographic factors include elevation, slope, vegetation, temperature, precipitation, and others^{22,23}. Studies have shown that changes in land use significantly affect HQ, with the expansion of construction land for industry, commerce, and residential areas leading to shifts in land use patterns that result in habitat degradation, particularly the decline of ecological forests and grasslands²⁴. However, owing to the complexity of ecosystems, HQ is shaped not only by land use changes but also by multiple interrelated factors^{19,25}. In natural environments, HQ is heavily influenced by topography, with higher elevations in mountainous regions generally associated with better HQ²⁶. Social factors, such as high population density and intensive mining activities, further exacerbate pressures on native species, resulting in habitat fragmentation and a prolonged decline in HQ²⁷. Thus, natural geographic factors establish the spatial variation in HQ, whereas economic and social factors drive temporal trends²⁸. Although previous studies have investigated these drivers individually, few have holistically examined their synergistic impacts over extended periods. Understanding the key drivers of HQ remains critical for formulating sustainable strategies in ecological planning and biodiversity conservation.

Against this backdrop, this study focuses on South Hunan, a region emblematic of China's resource-driven growth-ecology dilemma. In the past 30 years, the region has experienced considerable influxes of population, capital, and industry, driven by its abundant reserves of rare earth, manganese, and iron ores²⁹. This has led to the emergence of a resource-driven urban agglomeration, where mining and related chemical industries play a central role. However, as a critical source for multiple water systems and characterized by widespread hilly terrain, the region also has a highly sensitive and fragile ecological environment³⁰. The excessive extraction and mismanagement of mineral resources have caused severe damage to local natural habitats, leading to fragmentation and degradation. In response, local governments and enterprises have started regulating mining activities and implementing ecological restoration measures³¹. Nevertheless, balancing mining development with the improvement of HQ remains a pressing challenge because of the long-standing dominance of the mining economy. This study aims to (1) investigate the spatiotemporal patterns and dynamic trends of HQ in the South Hunan Mining Urban Agglomeration over the past 30 years; (2) predict future HQ scenarios for the region; and (3) analyze the primary drivers of HQ changes in the area. These analyses generate novel datasets and actionable insights to advance ecological planning in mining city clusters. This study not only addresses critical gaps in regional ecological security but also establishes a transferable framework for reconciling resource extraction with habitat conservation in global mining hotspots.

Materials and methods

Research area

The research area is situated in the southern portion of the middle Yangtze River Basin in China (Fig. 1), with geographical coordinates spanning from 109° 15' to 114° 40' E and 24° 25' to 27° 50' N, covering a total area of approximately 1.06×10^5 km². The region comprises 59 county-level cities and is characterized by terrain dominated by mountains and hills, serving as the source of multiple river systems. The region's climate is classified as a subtropical monsoon climate, with an annual precipitation of approximately 1200–1800 mm³². The South Hunan region is rich in mineral resources, including colored metals and nonmetallic minerals, with many deposits (such as tungsten, bismuth, rare earth, manganese, microcrystalline graphite, and fluorite) ranking among the top in the country in terms of reserves and grade³³. The primary industries in the region include the extraction and processing of colored metals and nonmetallic minerals, mineral smelting and extension, and the manufacture of chemical raw materials and products.

Data sources and processing

This study relies primarily on the following data sources: (1) Land use data were obtained from the Resource and Environment Science Data Center, Chinese Academy of Sciences (<http://www.resdc.cn>). This land use dataset adopts a two-level classification system, with the first level categorizing land into six types and the second level dividing land into 19 types (Table S1). (2) DEM data were sourced from the NASA-released SRTM global DEM (<https://lpdaac.usgs.gov/>), and the study area DEM was extracted via ArcGIS 10.8 software. (3) Meteorological data were obtained from the China Meteorological Data Network (<http://data.cma.cn/>), and the raster data

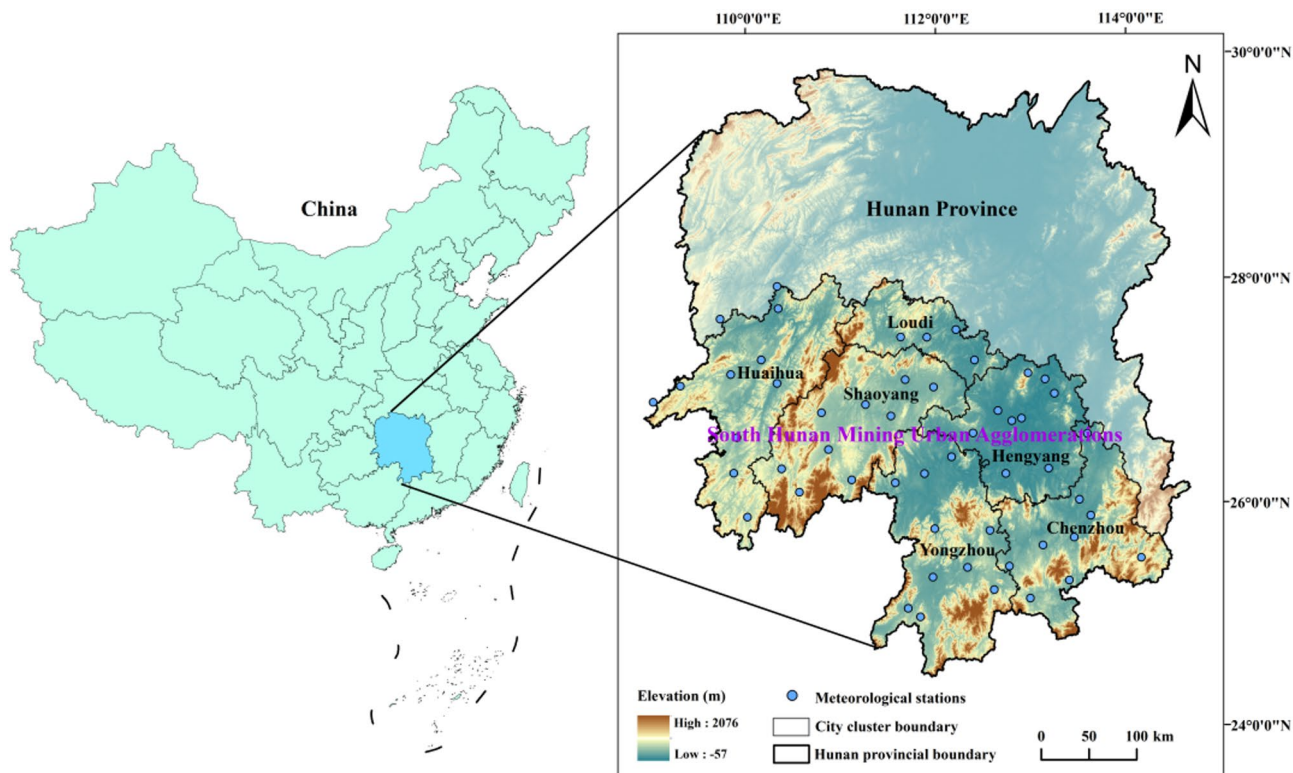


Fig. 1. Overview map of the study area. Generated in the ArcGIS 10.8 software (www.esri.com).

Data type	Original resolution	Processing	Data source
Land use data	30 m	Data for 1990, 1995, 2000, 2005, 2010, 2015, and 2020	The Resource and Environment Science Data Center, Chinese Academy of Sciences (http://www.resdc.cn)
DEM	30 m	The study area DEM was extracted via ArcGIS 10.8 software	The NASA-released SRTM global DEM (https://lpdaac.usgs.gov/)
Precipitation	Point data	Data for 1990, 1995, 2000, 2005, 2010, 2015, and 2020	The China Meteorological Data Network (http://data.cma.cn/)
Temperature			
River distribution	100 m	Data for 2000, 2005, 2010, 2015, and 2020	The Resource and Environment Science Data Center, Chinese Academy of Sciences (https://www.resdc.cn)
Road distribution	100 m	Data for 2000, 2010, and 2020	
Soil type data	1000 m	The study area soil type data was extracted via ArcGIS 10.8 software	
Population density	1000 m	Data for 1990, 1995, 2000, 2005, 2010, 2015, and 2020	
GDP	1000 m		
Mining industry data	Point data	Data for 1990–2020	The statistical yearbooks of the study area's municipalities and counties for the years 1990–2020
Nighttime light brightness	500 m	Data for 1990, 1995, 2000, 2005, 2010, 2015, and 2020	The National Tibetan Plateau Environment Data Center (https://data.tpdc.ac.cn)

Table 1. Data types, processes and sources.

were spatially interpolated by ArcGIS 10.8 software. (4) River distribution, road distribution, soil type data, population density and GDP data were sourced from the Resource and Environment Science Data Center, Chinese Academy of Sciences (<https://www.resdc.cn>). (5) Mining industry data were sourced from the statistical yearbooks of the study area's municipalities and counties for the years 1990–2020. (6) Nighttime light brightness data were obtained from the National Tibetan Plateau Environment Data Center (<https://data.tpdc.ac.cn>). Data types, original resolution, processes and sources are detailed in Table 1. Following preprocessing, all grid data were standardized to a 100 m × 100 m resolution and projected in the WGS_1984_Albers coordinate system.

Research framework

This study employed a systematic research framework (Fig. 2) integrating spatial analysis, scenario simulation, and statistical modeling to investigate the spatiotemporal dynamics of HQ and its drivers in the South Hunan Mining Urban Agglomeration. The workflow comprised four stages: (1) land use change analysis, (2) HQ

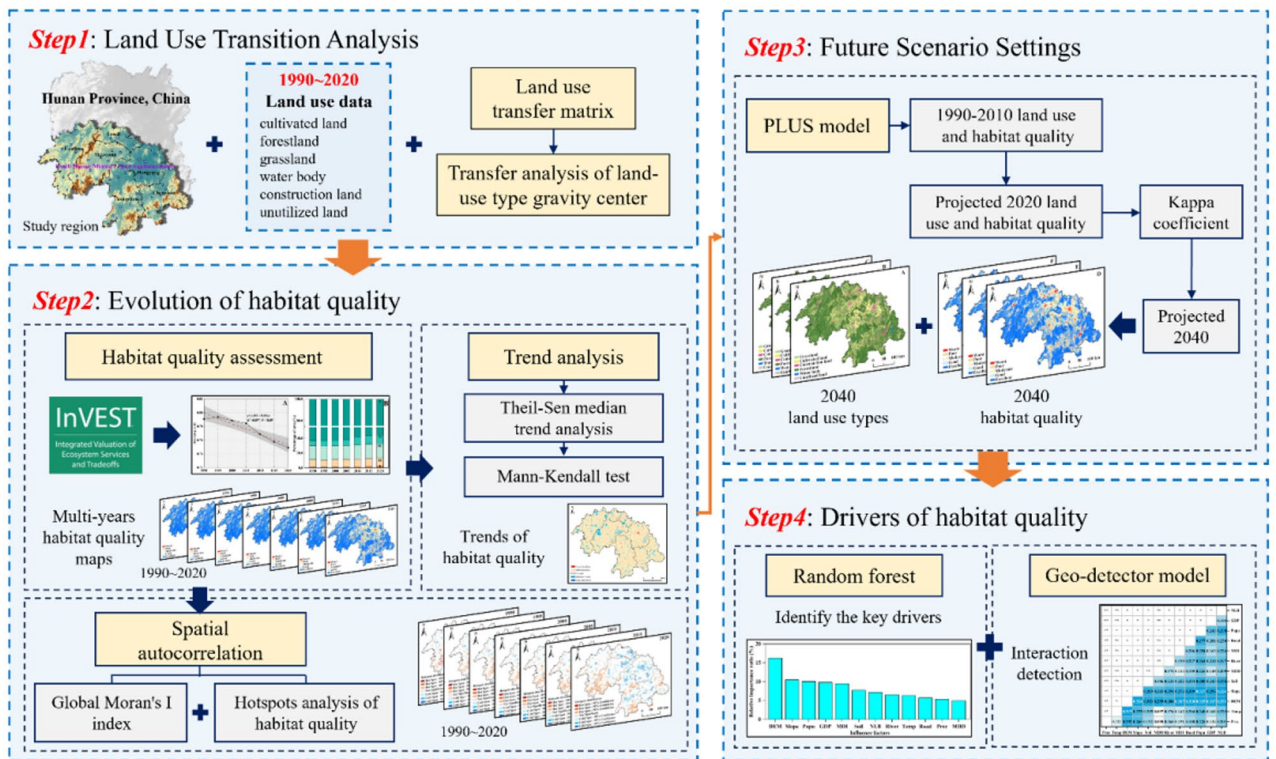


Fig. 2. Research framework.

assessment and trend quantification, (3) future scenario projections, and (4) driver identification. Below, we elaborate on each component, with justifications for model selection and parameterization.

Land use transition analysis

The land use transfer matrix is used to quantify the dynamic transitions and quantitative variations among land use categories³⁴. Theoretically grounded in Markov chain principles, this matrix formulation characterizes the state transition process of quasi-stable systems between discrete temporal intervals (from time K to $K + 1$), thereby providing spatiotemporal visualization of land use dynamics within the study area³⁵. This investigation employs the land use transfer matrix methodology to conduct a comprehensive analysis of land use transformations occurring in the study region during the 1990–2020 period.

The concept of the “center of gravity”, originating from physics, represents the equilibrium point of an object’s mass distribution³⁶. This principle has been extended to geographical studies to quantify the spatial concentration and dynamic shifts of land-use types³⁷. The gravity model can provide some insight into the distributional characteristics of spatial changes in land use types by analyzing the direction and distance of the shift in the center of gravity of each land use type³⁸. In this study, we employ centroid migration analysis of construction land to delineate the spatiotemporal evolutionary trajectory of urbanization patterns within the research area. By tracking the shifting coordinates of the center of gravity, we elucidate the directional bias and intensity of the expansion of mining city clusters.

Habitat quality assessment

We applied the InVEST model to evaluate HQ. The HQ index, which ranges from 0 to 1, reflects the ecological quality of an area, with higher values indicating better quality³⁹. The formula is as follows:

$$HQ_{xj} = H_{xj} \left(1 - \left(\frac{D_{xj}^z}{D_{xj}^z + k^z} \right) \right) \tag{1}$$

where HQ_{xj} represents the HQ of pixel x in land use type j ; H_{xj} denotes the habitat suitability of pixel x in land use type j ; z is a normalization constant; k is the half-saturation constant, typically set to 0.5; and D_{xj} indicates the degree of habitat degradation of pixel x in land use type j . The formula is as follows:

$$D_{xj} = \sum_1^R \sum_1^{Y_r} \left(\frac{w_r}{\sum_1^R w_r} \right) r_y i_{rxy} \beta_x S_{jr} \tag{2}$$

where i_{rxy} is the effect of threat factor r in image y on image x , w_r is the weight of the threat factor, r_y is the intensity of the threat factor, β_x is the resistance of the habitat to interference, and S_{jr} is the sensitivity of the different habitats to the different threat factors.

In this study, on the basis of the InVEST guidelines, which refer to the research of related scholars^{26,39–41} and synthesize the opinions of experts in the field of ecology for optimization, the final selection of cultivated land, urban land, rural settlements, other construction land, and unutilized land as threat factors, the weights of the factors and the distances of the impacts are shown in Table 2, and the suitability of the habitats and their sensitivity to the factors are shown in Table S2.

To more accurately describe the spatiotemporal changes in HQ in the South Hunan Mining Urban Agglomeration, we categorized the HQ grades into worst (0–0.2), worst (0.2–0.4), moderate (0.4–0.6), good (0.6–0.8), and excellent (0.8–1.0) grades on the basis of the actual situation of the study area via the reclassification tool of the ArcGIS 10.8 software platform.

Trend analysis

The Theil–Sen median trend analysis and Mann–Kendall test are commonly used to identify trends in long-term time series data⁴². The Theil–Sen method is a reliable nonparametric approach for trend estimation and is calculated via the following formula:

$$\beta = \text{median} \left(\frac{H_j - H_i}{j - i} \right) \quad (1990 \leq i \leq j \leq 2020) \tag{3}$$

where H_j and H_i represent the HQ values in years j and i , respectively, and β represents the trend of change in HQ; when $\beta > 0$, it indicates a decreasing trend in HQ; conversely, it indicates an increasing trend. The Mann–Kendall test is a nonparametric statistical test suitable for testing the significance of trends via the following formula⁴³:

$$S = \sum_{i=1}^{n-1} \sum_{j=i+1}^n \text{sgn}(H_j - H_i) \tag{4}$$

$$\text{sgn}(H_j - H_i) = \begin{cases} 1, & H_j - H_i > 0 \\ 0, & H_j - H_i = 0 \\ -1, & H_j - H_i < 0 \end{cases} \tag{5}$$

$$V_s = \frac{n(n-1)(2n+5)}{18} \tag{6}$$

$$Z = \begin{cases} \frac{S-1}{\sqrt{V_s}}, & S > 0 \\ 0, & S = 0 \\ \frac{S+1}{\sqrt{V_s}}, & S < 0 \end{cases} \tag{7}$$

where sgn represents the sign function, n is the number of data points in the time series, and V_s is the variance of the S statistic. At the α level, a significant trend in HQ is indicated if $Z > Z - \alpha/2$, with a commonly set at 0.05. If $|Z| > 1.96$, the trend is considered statistically significant at the 95% confidence level; otherwise, it is not⁴⁴.

Spatial autocorrelation

HQ has a certain regularity in spatial distribution, and spatial autocorrelation modeling can respond to the correlation between variables in a region and can be used to describe whether HQ has a clustering effect on the whole study area⁴⁵. In this study, the global Moran’s I index was used to estimate the degree of clustering of HQ via the following formula:

$$I = \frac{n \sum_{i=1}^n \sum_{j=1}^n \omega_{ij} (x_i - \bar{x})(x_j - \bar{x})}{S^2 \sum_{i=1}^n \sum_{j=1}^n \omega_{ij}} \tag{8}$$

Threat factors	Maximum influence distance (km)	Relative weight	Types of spatial decline
Cultivated land	1	0.7	Linear
Urban land	10	1.0	Exponential
Rural settlements	5	0.6	Exponential
Other construction land	8	0.7	Exponential
Unutilized land	1	0.5	Linear

Table 2. Maximum influenced distance and weight of threat factors.

where n represents the total number of grids, w_{ij} is the spatial weight matrix, and x_i and x_j are the HQ values of grids i and j , respectively. where \bar{x} is the average HQ value. Moran's I index quantifies spatial dependence by evaluating whether HQ are clustered (positive autocorrelation), dispersed (negative autocorrelation), or randomly distributed (no autocorrelation). A value closer to 1 indicates strong clustering of similar HQ values (e.g., hotspots of high HQ or coldspots of low HQ), while a value closer to -1 suggests spatial dispersion (e.g., alternating high and low HQ patches).

Cold hotspot analysis mainly uses the Getis-Ord G_i^* (G coefficient) provided by the Arc GIS platform to perform local statistics of spatial heterogeneity⁴⁶. This method helps identify statistically significant high and low values in the HQ distribution. Significantly positive G_i^* values indicate high aggregation and hotspots, whereas significantly negative G_i^* values suggest low aggregation and cold spots.

Future scenario projections

The PLUS model is an advanced land-use change simulation model developed on traditional cellular automata⁴⁷ and is composed of two major modules: the land expansion analysis strategy module and the Cellular Automata model, which is based on multiclass random seed blocks⁴⁸. The study simulated the land use situation in 2020. The overall simulation accuracy is 0.904, and the kappa coefficient is 0.863, indicating that the model parameters are reasonable (Table S3 and Fig. S1). On the basis of feasible conditions and future development requirements, this study subsequently establishes three distinct future scenarios for 2040:

Natural development scenario: This scenario simulates the South Hunan Mining Urban Agglomeration via the PLUS model, which is based on land use changes from 1990 to 2020, without considering additional constraints.

Ecological Protection Scenario: In this scenario, the South Hunan Mining Urban Agglomeration pursues green development and builds an ecologically friendly city group. The focus is on ecological protection, reducing resource development, and conserving regional biodiversity.

Economic development scenario: In this scenario, the South Hunan Mining Urban Agglomeration aims for economic growth and expansion of the industrial scale. It innovates and develops mining and related deep processing industries to drive economic development.

Random forest

The random forest model is based on decision tree classifiers and is capable of effectively handling various data types and assessing the importance of variables, thereby exhibiting strong predictive power^{49,50}. This study selected several environmental factors influenced by natural processes and human activities, including precipitation, temperature, DEM, slope, soil type, mineral distribution density, river distance, mining development index, road distance, population density, GDP, and nighttime light brightness. Using R software, a random forest analysis was conducted to identify the key drivers impacting the spatiotemporal changes in HQ within the study area.

Geodetector model

The geodetector model is a statistical approach used to identify the similarity in spatial differentiation among geographic elements and the factors driving the spatial variation in the dependent variable⁵¹. Its interaction detection module can further examine how different drivers interact to influence the spatial differentiation of HQ within a specific area⁵². In this study, we applied the interaction detection module of Geodetector to explore the roles and interactions of factors.

The factor detector quantifies the explanatory capacity of spatial determinants in accounting for HQ variance, operationalized through the q -value (0,1). This parametric metric demonstrates strict monotonicity, where higher values indicate greater explanatory power⁵³. The formula is as follows:

$$q = 1 - \frac{\sum_{h=1}^L N_h \sigma_h^2}{N \sigma^2} = 1 - \frac{SSW}{SST} \quad (9)$$

$$SSW = \sum_{h=1}^L N_h \sigma_h^2 \quad (10)$$

$$SST = N \sigma^2 \quad (11)$$

where h is a specific type, $h = 1, 2, \dots, L$ is the number of categories of variable Y or factor X ; N_h and N represent the number of h -category and the number of region-wide, respectively; and σ_h^2 and σ^2 represent the h -category and intra-region variance, respectively. SSW and SST are the sum of the variances of the L -categories and the total regional variance, respectively. The interactive detector identifies the interactions among different independent variables X , responding to whether the influence of two factors on Y is correlated or independent when acting together, and is derived from the q -value [$q(X_1 \cap X_2)$]⁵⁴ as shown in Table 3.

Results

Evolution of Spatial and Temporal patterns of land use types

The South Hunan Mining Urban Agglomeration exhibits diverse and complex land use patterns. From 1990 to 2020 (Table 4), forestland (over 66%) and cultivated land (approximately 26–28%) were the predominant land use types. Collectively, forestland and cultivated land occupied 93% of the study area, significantly influencing the overall landscape. Conversely, construction land, water bodies, and unutilized land constituted a minor fraction, only 7% of the total area. A key trend during this period was the decline in forestland, cultivated

Criterion of interval	Interaction
$q(X_1 \cap X_2) < \text{Min}[q(X_1), q(X_2)]$	Nonlinear weakening
$\text{Min}[q(X_1), q(X_2)] < q(X_1 \cap X_2) < \text{Max}[q(X_1), q(X_2)]$	Unilinear reduction
$q(X_1 \cap X_2) > \text{Max}[q(X_1), q(X_2)]$	Bilinear enhancement
$q(X_1 \cap X_2) = q(X_1) + q(X_2)$	Mutual independence
$q(X_1 \cap X_2) > q(X_1) + q(X_2)$	Nonlinear enhancement

Table 3. Model driving force size criterion of interval and interaction.

Land use types		Cultivated land	Forestland	Grassland	Water body	Construction land	Unutilized land
1990	Area	29544.31	71260.78	3226.10	1146.12	933.87	10.61
	Ratio	27.84	67.15	3.04	1.08	0.88	0.01
1995	Area	29151.66	71430.58	3183.65	1273.46	1061.22	21.22
	Ratio	27.47	67.31	3.00	1.20	1.00	0.02
2000	Area	29342.67	71101.60	3194.27	1390.20	1071.83	21.22
	Ratio	27.65	67.00	3.01	1.31	1.01	0.02
2005	Area	29215.33	71112.21	3183.65	1400.81	1188.56	21.22
	Ratio	27.53	67.01	3.00	1.32	1.12	0.02
2010	Area	28801.45	71218.33	3003.25	1432.64	1655.50	21.22
	Ratio	27.14	67.11	2.83	1.35	1.56	0.02
2015	Area	28652.88	71133.43	2971.41	1432.64	1910.19	21.22
	Ratio	27.00	67.03	2.80	1.35	1.80	0.02
2020	Area	28419.41	70984.86	2939.57	1453.87	2313.45	10.61
	Ratio	26.78	66.89	2.77	1.37	2.18	0.01

Table 4. Area (km²) and ratio (%) of land use types in mining urban agglomerations from 1990–2020.

land, and grassland within the region, while construction and water body areas steadily increased. Notably, the construction land area expanded considerably, from 933.87 km² in 1990 to 2313.45 km² in 2020.

Figure 3 illustrates the dynamics of land use changes in the South Hunan Mining Urban Agglomeration. From 1990 to 1995, alterations predominantly occurred between cultivated land, grassland, and forestland, with the largest reciprocal exchange observed between cultivated land and forestland, followed by a 277.90 km² transfer from grassland to forestland. In the subsequent periods from 1995 to 2000 and from 2000 to 2005, the transfer between cultivated land and forestland continued to exhibit the most significant changes, with the inflow and outflow of these two land types largely balanced. From 2005 to 2010, the areas converted from cultivated land to forestland and from forestland to cultivated land were 2015.01 km² and 1940.23 km² respectively. Additionally, 638.10 km² of both cultivated land and forestland were converted to construction land, indicating a crucial shift in resource availability. From 2010 to 2015, the area of mutual transfer between cultivated land and forestland exceeded 3000 km² highlighting substantial fluctuations in these resources within the region. Finally, from 2015 to 2020, the conversions of cultivated land and forestland to construction land reached 501.71 km² and 369.83 km² respectively, highlighting a pivotal phase for construction land expansion. Therefore, the expansion of construction land has originated primarily from reductions in cultivated and forest lands, with the decline in forestland largely driven by reciprocal changes with cultivated land.

Analyzing the spatial changes in construction land reveals the urbanization pattern of the South Hunan Mining Urban Agglomeration. We examined the distribution of the center of gravity of construction land in the study area from 1990 to 2020 via the standard deviation ellipse method. As shown in Fig. 4, the center of gravity followed a recurring southeast–northwest movement, with the ratio of the long axis to the short axis of the standard deviation ellipse initially decreasing and then increasing. Specifically, in 1990, 1995, and 2000, the center of gravity was concentrated in the middle, with long-to-short axis ratios of 1.615, 1.617, and 1.609, respectively. By 2005, it had shifted northwestward, with the ratio reaching 1.617. In 2010, the center moved southeast again, causing the ratio to decrease to 1.575. In 2015 and 2020, the center shifted back northwest, with the ratio increasing to 1.631 and 1.646, respectively. This suggests that the mining urban agglomeration is transitioning toward a more dispersed development model.

Evolution of spatial and temporal patterns of HQ

Figure 5 shows that the average HQ in the South Hunan Mining Urban Agglomeration ranged from 0.72 to 0.82 between 1990 and 2020, indicating that an overall high level of ecological quality was sufficient to support biodiversity. However, a significant trend of initial increase followed by a sustained decline ($R^2 = 0.897$) was observed. The maximum was recorded in 1995 (0.794), whereas the minimum was observed in 2020 (0.749).

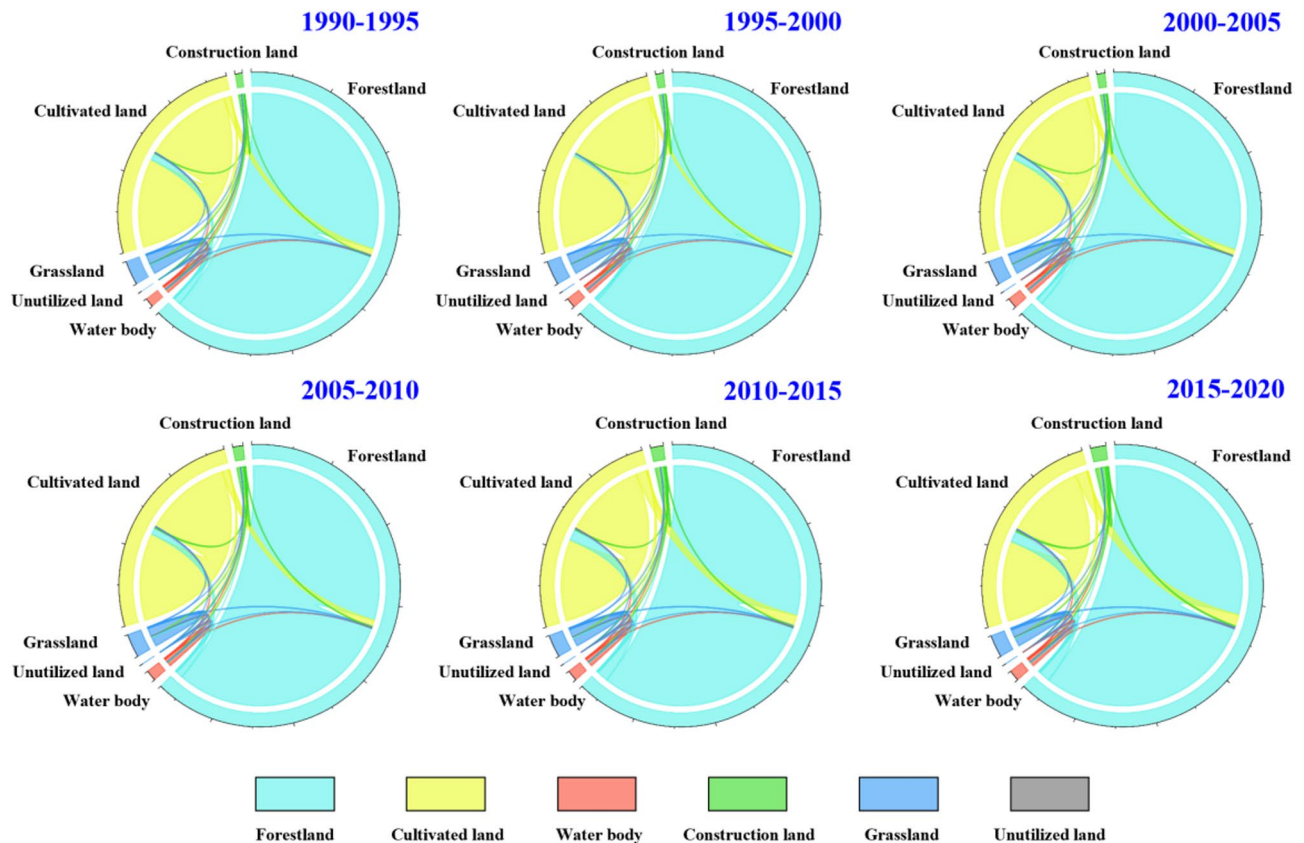


Fig. 3. Land use transfer in mining urban agglomeration from 1990 to 2020. Changes in the color scale of the figure indicate the area transferred between different land-use types.

The area of different grades of HQ in the South Hunan Mining Urban Agglomeration from 1990 to 2020 also underwent large temporal changes (Fig. 5). The results revealed that the area proportion of the excellent grade of HQ was as high as 63.8% and 63.71% in 1990 and 1995, respectively, in the South Hunan Mining Urban Agglomeration; however, the area proportion of the excellent grade continued to decrease over time, and the area proportion of the excellent grade decreased to 54.80% in 2020. In addition, the greatest change was in the proportion of good-grade HQ areas, which increased in volatility from 6.62% in 1980 to 12.63% in 2020. In contrast, the proportion of areas in the moderate, poor, and worst grades only slightly increased between 1990 and 2020.

The spatial distribution of HQ in the South Hunan Mining Urban Agglomeration from 1990 to 2020 revealed an overall distribution pattern of lower HQ in the center and higher HQ in the surrounding areas (Fig. 6). Specifically, the central part of Hengyang, the central part of Loudi, and the northern part of Shaoyang have a spatial distribution pattern of lower HQ and are clustered. On the other hand, high HQ were distributed mainly in Huaihua, southern Shaoyang, and central and southern Yongzhou but with a decentralized spatial distribution. In addition, after 2010, patches with lower HQ in central Hengyang, central Loudi, and northern Shaoyang showed an expanding distribution trend, indicating that habitat fragmentation and degradation in these areas gradually increased.

The trend analysis of HQ in the South Hunan Mining Urban Agglomeration from 1990 to 2020 revealed (Fig. 7) that 93.58% of the area of the study area tended to degrade HQ, among which a serious degradation trend occurred in the central part of Hengyang, Chenzhou, the northern part of Shaoyang, and Yongzhou, which accounted for 0.80% of the area of the study area. Moreover, the area with improved HQ is only 6815.40 km² which is distributed mainly in the intersection area of Huaihua, Yongzhou, and Loudi, among which the HQ of approximately 19.71 km² in the central part of Huaihua has a strong trend of improvement, accounting for 0.02% of the study area.

Spatial correlation characteristics of HQ

We employed the global Moran's I index to analyze the spatial association features of the HQ in the South Hunan Mining Urban Agglomeration (Table 5). We established a 4 × 4 km grid for the study area and allocated the HQ within each grid cell on the basis of the average values. The results revealed that the annual global Moran's I indices for the study area from 1990 to 2020 ranged from 0.296 to 0.365, all of which were significantly greater than 0. This indicated that there was positive spatial autocorrelation and agglomeration of HQ, reflecting the continued aggregation of degraded habitats in the central region and high-quality habitats in the surrounding

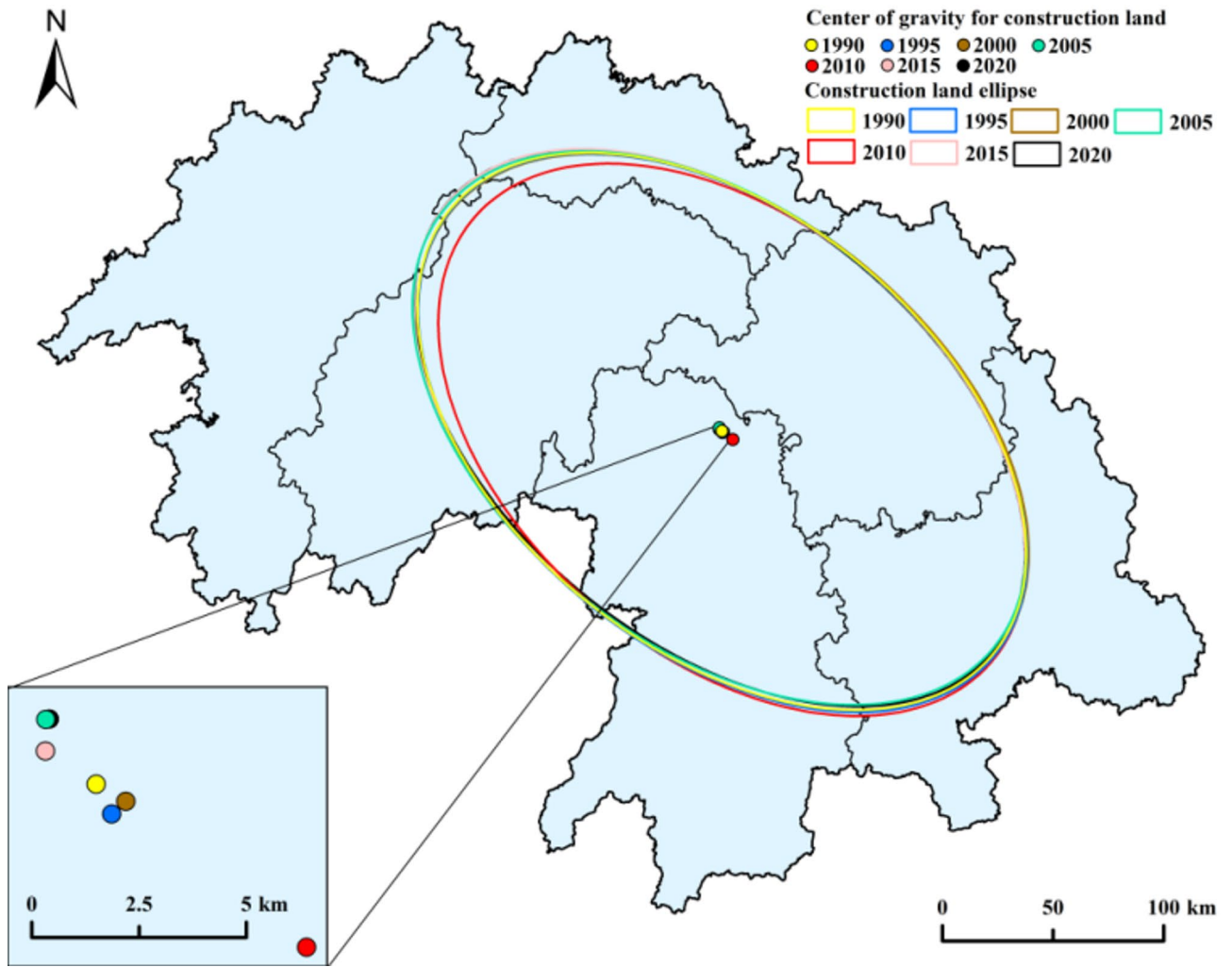


Fig. 4. Transfer trajectories of the center of gravity of construction land and standard deviational ellipse in mining urban agglomeration from 1990 to 2020. Generated in the ArcGIS 10.8 software (www.esri.com).

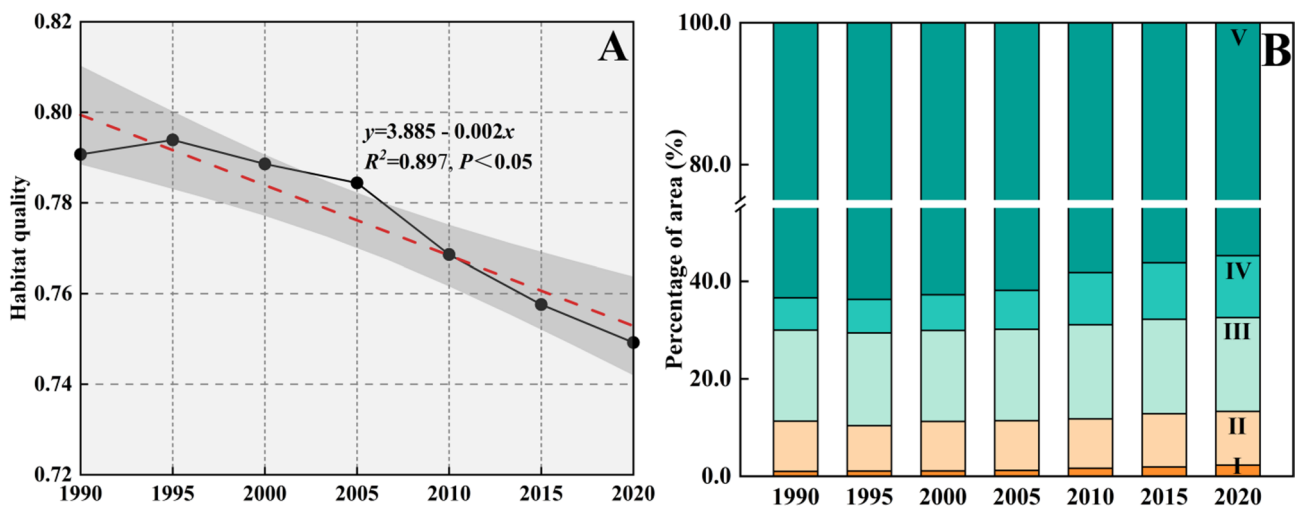


Fig. 5. Temporal changes in HQ (A) and changes in the area of different grades of HQ (B) in mining urban agglomeration from 1990 to 2020. I: Worst; II: Poor; III: Moderate; IV: Good; V: Excellent.

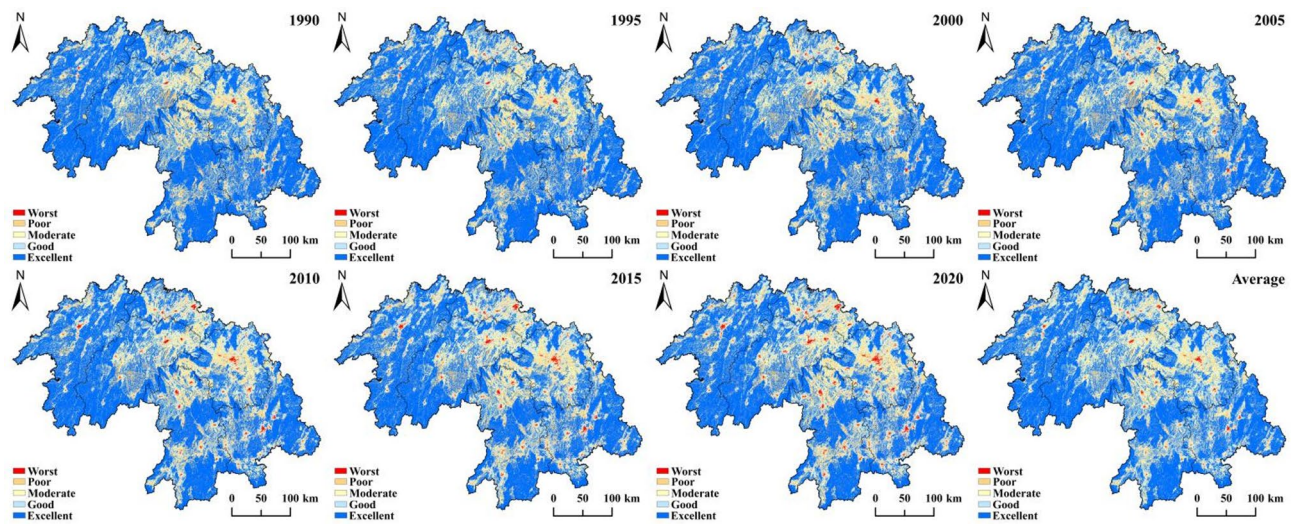


Fig. 6. Spatial pattern of HQ in mining urban agglomeration from 1990 to 2020. Generated in the ArcGIS 10.8 software (www.esri.com).

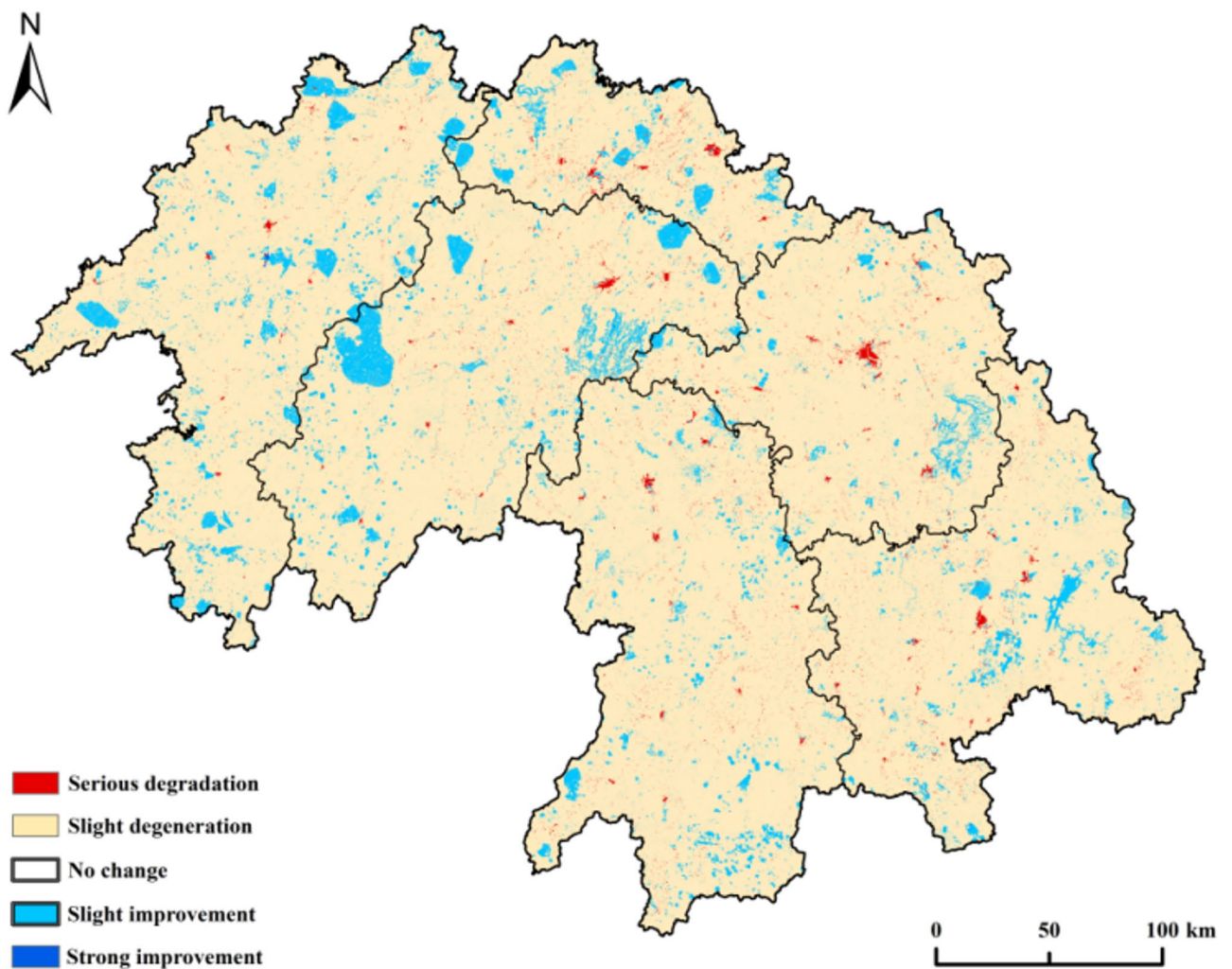


Fig. 7. Trends of HQ in mining urban agglomeration from 1990 to 2020. Generated in the ArcGIS 10.8 software (www.esri.com).

Year	1990	1995	2000	2005	2010	2015	2020
Moran's I	0.296	0.301	0.305	0.317	0.344	0.339	0.365
Z score	33.643	34.210	34.691	35.986	39.103	38.507	41.464
P value	0.000	0.000	0.000	0.000	0.000	0.000	0.000

Table 5. Moran's I index values of HQ in mining urban agglomerations from 1990–2020.

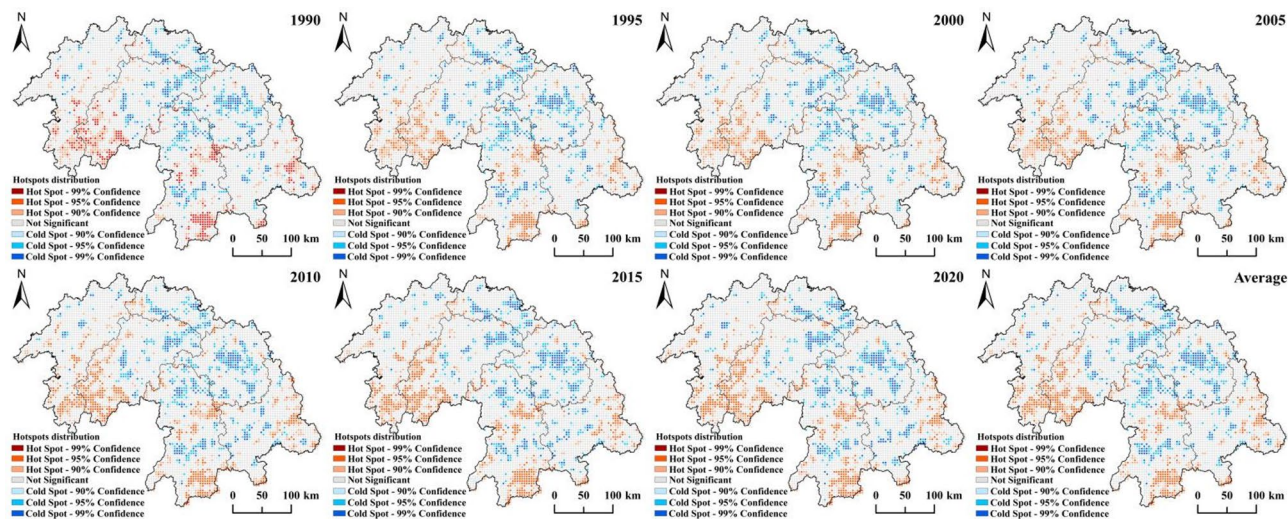


Fig. 8. Hotspots analysis of HQ in mining urban agglomeration from 1990 to 2020. Generated in the ArcGIS 10.8 software (www.esri.com).

mountains. Furthermore, the *Z scores* were consistently above 2.58, and the *P values* were below 0.01, confirming that the global Moran's I index is significant at the 1% confidence level. Moreover, the index increased from 0.296 in 1990 to 0.365 in 2020, indicating that habitat degradation is increasingly concentrated in specific areas under the pressure of urbanization and industrial and mining development.

Figure 8 shows the spatial distributions of HQ hotspots and coldspots in the South Hunan Mining Urban Agglomeration from 1990 to 2020. During this period, the hotspots of HQ in the study area were primarily concentrated in the Huaihua, southern Shaoyang, and southeastern Yongzhou and Chenzhou regions. These areas are rich in mountainous forest resources and have good ecological environments, serving as the main sources of high HQ for the South Hunan Mining Urban Agglomeration. In contrast, the cold spots of HQ were located mainly in the plains and low hill areas of central and northern Shaoyang, Loudi, Hengyang, and Yongzhou. Frequent mining activities, expansion of construction land, and agricultural cultivation in these areas may have contributed to the clustering of low HQ zones. Furthermore, over the past 30 years, the proportions of cold spots in the study area were 14.69% (1990), 14.87% (1995), 14.79% (2000), 15.14% (2005), 15.50% (2010), 14.99% (2015), and 15.08% (2020), indicating a gradual increase in the extent of low HQ clusters.

Future scenario projections of HQ

As shown in Fig. 9, under the three development scenarios, the spatial distribution of land use in the South Hunan Mining Urban Agglomeration in 2040 is consistent with the characteristics of 2020 and is still dominated by cultivated land and forestland, with forestland being the most extensive. Under the natural development scenario, construction land expanded significantly beginning in 2020, with an increase of 872.90 km² and a significant decrease in the area of cultivated land and grassland. Under the ecological protection scenario, forestland expanded significantly beginning in 2020, with an increase of 1283.49 km² whereas the area of construction land increased by only 69.77 km². Under the economic development scenario, construction land expanded significantly from 2020, with an increase of 1229.78 km² and the areas of cultivated land and grassland decreased by 130.82 and 1116.04 km² respectively.

Under the three development scenarios, the HQ of the South Hunan Mining Urban Agglomeration exhibited a distribution pattern characterized by lower quality in the center and higher quality in the surrounding areas, which was consistent with the observations from 2020 (Fig. 9). Under the natural development scenario, the average HQ was 0.738, with the area of the worst-grade patches increasing by 875.35 km² compared with that in 2020. These patches were located primarily in the central cities and surrounding townships of Shaoyang, Hengyang, and Yongzhou, indicating that the unchecked expansion of construction land has led to habitat degradation. Conversely, under the ecological protection scenario, which prioritized ecological conservation and limited resource development, the average HQ improved slightly to 0.743. In this scenario, the area of the worst grade patches increased by only 84.05 km² compared with that in 2020, suggesting that ecological

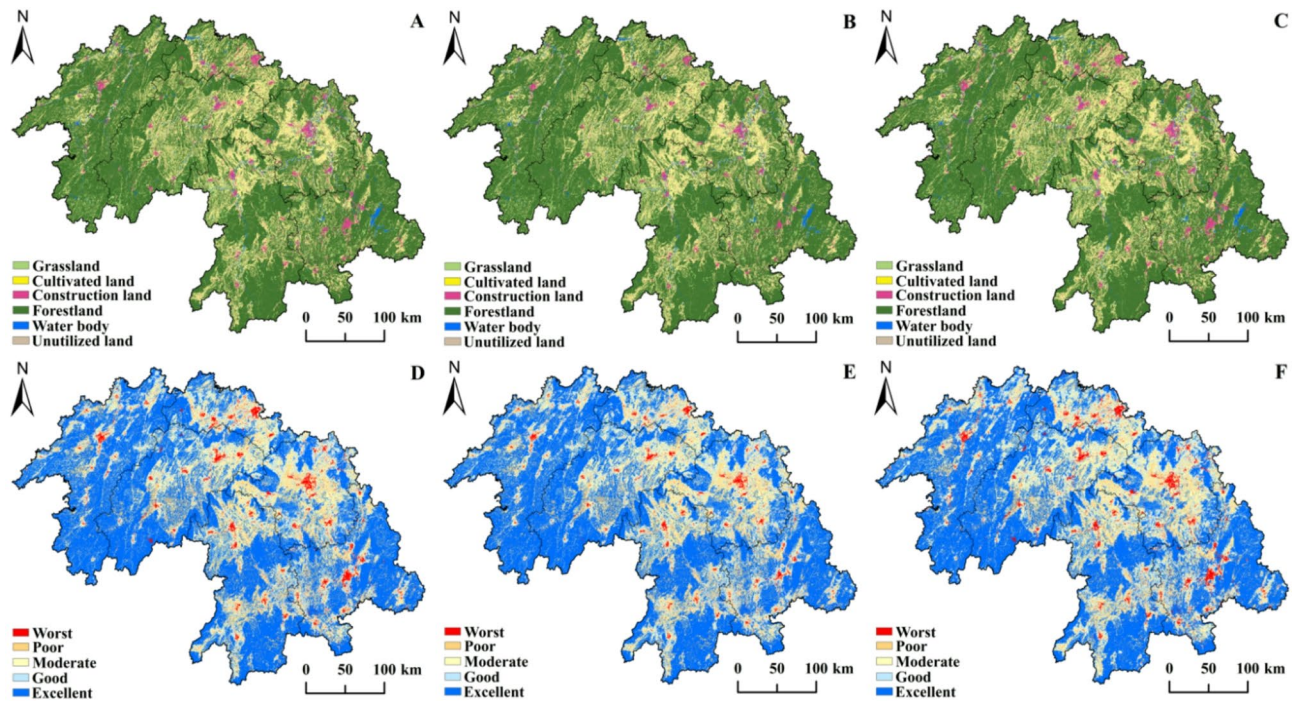


Fig. 9. Simulation of spatial distribution of land use types (ABC) and HQ (DEF) under different scenarios for mining urban agglomeration in 2040. (A,D) natural development scenario; (B,E) ecological protection scenario; (C,F) economic development scenario. Generated in the ArcGIS 10.8 software (www.esri.com).

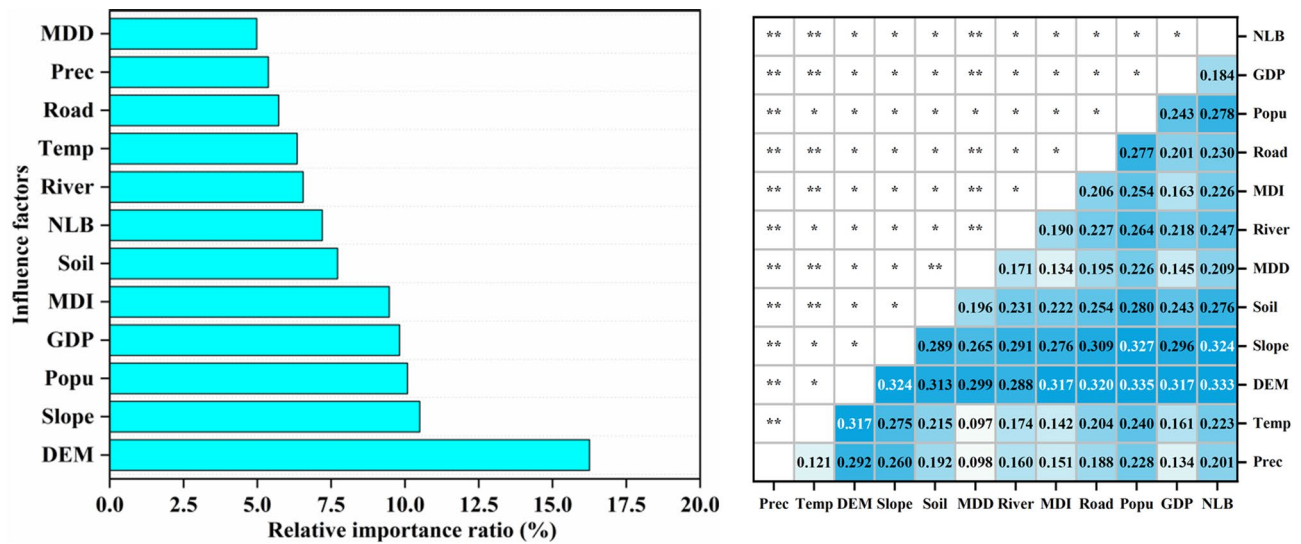


Fig. 10. (A) Importance of influencing factors the HQ. (B) Interactions in drivers of HQ. *Bilinear enhancement. **Nonlinear enhancement. *Prec* precipitation, *Temp* temperature, *Soil* soil type, *MDD* mineral distribution density, *River* river distance, *MDI* mining development index, *Road* road distance, *Popu* population density, *NLB* nighttime light brightness.

management measures effectively mitigated habitat degradation. Under the economic development scenario, the average HQ declined to 0.726, with the area of the worst grade patches increasing significantly by 1240.26 km² relative to the other two scenarios, whereas the area of the excellent grade patches decreased markedly.

Drivers of spatial and temporal patterns of HQ

We utilized the mean decrease accuracy (MDA) method to obtain the importance ranking of the influencing factors of the random forest classification. The results are shown in Fig. 10. The three drivers influencing the spatiotemporal patterns of HQ in the South Hunan Mining Urban Agglomeration were DEM, slope and Popu

(population density). Specifically, topographic and geomorphic factors such as elevation and slope significantly drove the spatial and temporal distributions of HQ in the study area, followed by anthropogenic factors such as population concentration (Popu) and industrial and mining development (MDI).

The Geodetector factor interaction (Fig. 10) revealed that the driver interaction in the study area mainly exhibited nonlinear enhancement and bilinear enhancement, with no instances of mutual independence or reduction observed. Among them, the interaction between Popu and the DEM was the most obvious, with an explanatory power of 0.335, indicating that the interaction between the two significantly affected the spatial pattern of HQ in the study area. Moreover, the explanatory power of the interaction between the NLB and the DEM, Popu and Slope was also high, at 0.333 and 0.327, respectively. Furthermore, the explanatory power of the interaction between the NLB and slope, slope and DEM, and road and DEM was ≥ 0.320 . Notably, the interaction between the MDI and DEM reached an explanatory power of 0.317. These results suggest that the spatial variation in HQ in the South Hunan Mining Urban Agglomeration was influenced mainly by the interaction of factors such as topography and geomorphology, human growth, and economic activities.

Discussion

This study employed a suite of analytical methods, including the InVEST model, PLUS model, random forests, and geodetector, to comprehensively assess the spatial and temporal dynamics of HQ within the South Hunan Mining Urban Agglomeration. We analyzed both historical trends and projected future scenarios. Furthermore, we investigated the key drivers influencing HQ. These findings are crucial for informing ecologically sound land-use policies and promoting the sustainable development of mining urban agglomerations.

Response of HQ to land use type change

The InVEST model evaluates the spatial and temporal changes in regional HQ, primarily using land-use data as its input source⁵⁵. The results of studies in the Loess Hilly Gully region and the Swiss Alps have shown that land use change affects ecosystem dynamics^{56,57} and that land use type is a key factor in determining the ecological carrying capacity of a region and influences the distribution patterns of different ecosystems⁵⁸. Thus, the spatiotemporal pattern of HQ mirrors the process of land use transformations driven by socioeconomic development¹². Similar to the findings on landscape fragmentation in traditional orchard systems of central Germany, where urban construction land expansion has been shown to disrupt multi-functional ecological pattern, our study highlights that construction land expansion in the South Hunan Mining Urban Agglomeration acts as a critical pressure axis, reducing regional ecological carrying capacity^{58,59}. The primary land-use types in the South Hunan Mining Urban Agglomeration are cultivated land and forestland, which significantly affect the overall landscape (Table 2). However, since 1990, forested land and cropland have decreased by 148%. In contrast, the area of construction land continued to increase with economic development and urban expansion (Fig. 3), which was basically consistent with the temporal trend of the HQ of the study area increasing and then continuing to decrease from 1990 to 2020 and the continuous expansion of patches of lower HQ (Fig. 5).

HQ exhibited a strong spatial correlation with land use patterns (Figs. 6, 7 and 8). High HQ was observed in the northwestern and southwestern portions of the study area, largely attributed to the predominance of forested land, complex forest ecosystem structure, and relatively low human impact. Conversely, the central and northeastern areas displayed significant habitat degradation, characterized by a dense distribution of low-quality patches. This degradation is likely driven by the concentration of urban and rural settlements, which primarily consist of construction land and cultivated land. The aggregation of cultivated land and the growth of construction areas have decreased habitat connectivity, intensifying habitat fragmentation⁶⁰ similar to findings in other landscapes^{61,62}. Furthermore, agricultural settlements, population density, and industrial activities such as mining and chemical production consume significant amounts of natural resources and generate substantial pollution, causing ecosystem damage and resulting in HQ decline^{63,64}.

In addition, projections for all three future scenarios (Fig. 9) indicated a decline in HQ compared with that in 2020, with varying increases in the areas of very poor-quality patches. This is consistent with research that generally recognizes that sprawling development tends to lead to habitat degradation^{65,66}. This highlights the region's vulnerability to habitat degradation. Future expansion of construction land and encroachment on forests and farmland are likely to accelerate this decline, particularly given the status of the study area as a typical industrial-mining urban agglomeration. Within this context, the development of the mining, smelting, and chemical industries poses a significant threat to HQ, exceeding the impact of agricultural resettlement and cultivated land expansion.

Drivers of spatial and temporal changes in HQ

This study employed random forest and geodetector analyses to investigate the drivers of spatial and temporal HQ dynamics within the South Hunan Mining Urban Agglomeration (Fig. 10). Our findings revealed that elevation (DEM), slope, population density, GDP, and the mining development index (MDI) all exhibited relative importance values exceeding 9.4%, and significant interactions with other factors were observed.

The southern Hunan mining urban agglomeration is located in the hilly region of south-central China, where elevation and slope are major constraints to human activities and have a strong influence on HQ, consistent with global studies correlating elevation gradients and habitat resilience^{11,67}. For example, a study in Ontario, Canada, found that elevation factors significantly influenced Dynamic habitat index⁶⁸ similar to what we found in southern Hunan, where high elevation maintained high HQ despite pressure from mining development. Human settlements and economic development in the South Hunan Mining Urban Agglomeration are concentrated in low-elevation, gently sloping areas, resulting in lower HQ. Conversely, steeper areas maintain relatively higher HQ due to reduced human impact and prevalent forest cover, highlighting the direct influence of topography on spatial HQ variation.

The population density, GDP, mining development index, and nighttime light intensity showed significant nonlinear positive interactions with topographic factors, which highlights the compound effect of industrialization and topography in mountainous mining areas. High population density, high GDP, and intense nighttime lighting result in intensive human activity, potentially leading to habitat loss, pollution, and reduced ecosystem functioning within parts of the cluster^{69–71}. The mining development index, in particular, directly reflects the negative impacts of the mining, smelting, and processing industries on land use, soil erosion, and heavy metal contamination⁷² thus contributing to a decreased HQ. As an urban agglomeration dominated by the mining industry, we observed that the mining development index had a less significant effect than did the interactions between population density and GDP. This could be attributed to the fact that open-pit and shallow mineral extraction may negatively affect surface habitat quality, whereas deep underground mining tends to have a more direct impact on deep groundwater and soil, with a slower influence on surface habitats⁷³. However, we note that this possibility phenomenon has been relatively understudied in existing mining habitat conservation frameworks and deserves further in-depth exploration. Additionally, as mining and smelting technologies advance, the implementation of precision mining methods, mine reclamation efforts, and pollutant control measures could help mitigate fluctuations in habitat quality, reducing their overall impact^{10,74}. In addition, we observed significant interactions of temperature, precipitation, and mineral distribution density with elevation and slope that showed a bilinear enhancement, reflecting the fact that the quality of mountain mining habitats may also be protected and limited by the coupling of climate, resource distribution, and topographic factors.

In conclusion, our results suggest that the spatial and temporal patterns of HQ in the South Hunan Mining Urban Agglomeration are mainly directly influenced by topographic factors such as DEM and slope. Meanwhile, the interactions between anthropogenic factors, including population density, GDP, and mining development index, and topographic factors further reflect that urbanization and industrialization development have exacerbated habitat pressure in fragile terrain, and thus we emphasize the need for spatially targeted habitat conservation.

Innovations and shortcomings of this study

This study investigated the evolutionary dynamics of land use and HQ in the South Hunan Mining Urban Agglomeration from 1990 to 2020. We employed a suite of methods, including land use transfer matrices, the InVEST model, trend analysis, and spatial autocorrelation, to analyze spatial and temporal patterns. Furthermore, we projected land use and HQ for 2040 under three scenarios via a combined PLUS-InVEST model. The driving factors of HQ dynamics were explored via random forests and geo-probes. By explicitly considering the region's unique characteristics as an industrial and mining urban agglomeration and integrating data on mineral distribution and industrial development into our driver assessment model, our findings provide a more comprehensive understanding of HQ changes and a more robust scientific basis for sustainable development planning in the South Hunan Mining Urban Agglomeration.

However, this study has several limitations. First, data acquisition in the South Hunan Mining Urban Agglomeration, a region with potentially high ecological risk, presented challenges. The scarcity of long-term, continuous environmental monitoring and socioeconomic data potentially limits the accuracy and reliability of our results. Second, future projections, which are based on scenario simulations, inherently involve assumptions and parameters subject to uncertainty, potentially introducing bias. The influence of future policy changes and socioeconomic developments on HQ is significant but difficult to fully incorporate into scenario simulations, leading to model imperfections. In addition, the reliance on 100 m resolution raster data may overlook fine-scale fragmentation, a limitation highlighted in a study in the Zagros Mountains where 10 m resolution raster data better resolved landscape function indices⁷⁵. Therefore, future research should focus on extending the modeling framework, refining parameters, enhancing the indicator system, and finer resolution raster data to more robustly explore spatial and temporal patterns and driving mechanisms of HQ at multiple spatial and temporal scales.

Suggestions

By coupling the PLUS and InVEST models, we established a dynamic framework to simulate HQ under contrasting development scenarios, addressing gaps in mining urban agglomeration studies that often overlook spatially explicit interactions between industrial expansion and habitat degradation. While prior research emphasized land use change as the primary HQ driver, our geodetector analysis revealed that topography moderates human impacts particularly population density that exacerbates habitat loss at low elevations. This refines theoretical models of ecological vulnerability in mountainous mining regions. The findings advocate for zoning policies that restrict construction land expansion in ecologically sensitive low-elevation plains. Scenario projections suggest prioritizing the ecological protection scenario, which limits HQ decline to 0.743, offering a viable pathway to balance mining economies with habitat integrity. Local governments should enforce stricter mining reclamation regulations and incentivize agroforestry in degraded areas. Urban planners must integrate HQ hotspots into ecological redlines to prevent fragmentation. Researchers should focus on long-term monitoring of the interactive effects of nighttime light intensity, slope and other factors to refine the complete assessment of HQ.

Conclusions

This study examined the spatial and temporal changes in land use and HQ from 1990 to 2020 in the South Hunan Mining Urban Agglomeration, projected future HQ scenarios for 2040, and identified key drivers of HQ dynamics. The key findings: (1) From 1990 to 2020, forestland and cultivated land dominate (93% combined), but construction land increases by 148%, with construction land replacing mainly forestland and cultivated land. At

the same time, the trajectory of the centre of gravity of construction land shows a trend of “southeast–northwest” movement, and a shift from centralized mining-driven clusters to decentralized urban sprawl, reflecting intensifying pressures of industrialization and urbanization. (2) Over the period from 1990 to 2020, the average HQ in the study area ranged from 0.72 to 0.82, with an initial increase followed by a decline. HQ was generally lower at the center of the study area and higher at the periphery, with high-quality habitats being dominant. However, the area of low-quality habitats gradually expanded. Notably, global Moran's I indices (0.296–0.365) confirmed strong spatial autocorrelation, highlighting persistent clustering of degraded habitats. (3) By 2040, all scenarios (natural development, ecological protection, economic development) predict further HQ declines. Under the economic development scenario, worst-grade habitats will increase by 1240.26 km² underscoring the ecological cost of unregulated mining and urban expansion. (4) Topography (DEM, slope) and human activities (population density, nighttime light intensity) synergistically shaped HQ. Interactions between population density and elevation (explanatory power: 0.335) dominated, emphasizing the compounded effects of anthropogenic pressures on fragile ecosystems. Our findings provide critical guidance for sustainable land-use planning and ecological management in the South Hunan Mining Urban Agglomeration. Prioritizing ecological conservation measures is vital to mitigate degradation and enhance habitat quality. We urge policymakers to integrate these insights into strategies that balance economic growth with biodiversity preservation. Meanwhile, future studies could incorporate high-resolution pollution data on heavy metal concentrations, socio-economic survey data combined with macro-ecological modeling, which may enhance the realism of the HQ assessment and simulation scenarios, and thus better predict the HQ changes in mining city clusters.

Data availability

The data that support the findings of this study are available from the corresponding author upon reasonable request.

Received: 1 January 2025; Accepted: 2 June 2025

Published online: 18 August 2025

References

- Dai, X. et al. Ecological vulnerability assessment of a china's representative mining City based on hyperspectral remote sensing. *Ecol. Ind.* **145**, 663. <https://doi.org/10.1016/j.ecolind.2022.109663> (2022).
- Shen, H. & Liu, Y. *Circular Economy Legislation and Environmental Pollution: Evidence from Urban Mining Pilot Cities in China* (2020).
- Yu, J., Zhang, Z. & Zhou, Y. The sustainability of china's major mining cities. *Resour. Policy*. **33**, 12–22 (2008).
- Moulatlet, G. M. et al. A systematic review on metal contamination due to mining activities in the Amazon basin and associated environmental hazards. *Chemosphere* **339**, 139700–139700. <https://doi.org/10.1016/j.chemosphere.2023.139700> (2023).
- du Preez, G., Wepener, V. & Dennis, I. Metal enrichment and contamination in a karst cave associated with anthropogenic activities in the Witwatersrand basin, South Africa. *Environ. Earth Sci.* **75**, 2. <https://doi.org/10.1007/s12665-016-5455-2> (2016).
- Bai, L., Xiu, C., Feng, X. & Liu, D. Influence of urbanization on regional habitat quality: a case study of Changchun City. *Habitat Int.* **93**, 42. <https://doi.org/10.1016/j.habitatint.2019.102042> (2019).
- Li, W., Wang, Y., Xie, S. & Cheng, X. Coupling coordination analysis and Spatiotemporal heterogeneity between urbanization and ecosystem health in Chongqing municipality, China. *Sci. Total Environ.* **791**, 311. <https://doi.org/10.1016/j.scitotenv.2021.148311> (2021).
- Hillard, E. M., Nielsen, C. K. & Groninger, J. W. Swamp rabbits as indicators of wildlife habitat quality in Bottomland hardwood forest ecosystems. *Ecol. Ind.* **79**, 47–53. <https://doi.org/10.1016/j.ecolind.2017.03.024> (2017).
- Xie, X. & Zhu, Q. Research on the impact of urban expansion on habitat quality in Chengdu. *Sustainability* **15**, 271. <https://doi.org/10.3390/su15076271> (2023).
- Zhang, H., Wang, F., Zhao, H., Kang, P. & Tang, L. Evolution of habitat quality and analysis of influencing factors in the yellow river Delta wetland from 1986 to 2020. *Front. Ecol. Evol.* **10**, 914. <https://doi.org/10.3389/fevo.2022.1075914> (2022).
- Xiao, P., Zhou, Y., Li, M. & Xu, J. Spatiotemporal patterns of habitat quality and its topographic gradient effects of Hubei Province based on the invest model. *Environ. Dev. Sustain.* **25**, 6419–6448. <https://doi.org/10.1007/s10668-022-02310-w> (2023).
- Zhang, X. et al. Spatial pattern reconstruction of regional habitat quality based on the simulation of land use changes from 1975 to 2010. *J. Geog. Sci.* **30**, 601–620. <https://doi.org/10.1007/s11442-020-1745-4> (2020).
- Lee, D. J. & Jeon, S. W. Estimating changes in habitat quality through land-use predictions: case study of roe deer (*Capreolus pygargus tianschanicus*) in Jeju Island. *Sustainability* **12**, 123. <https://doi.org/10.3390/su122310123> (2020).
- Yang, Y. Evolution of habitat quality and association with land-use changes in mountainous areas: A case study of the Taihang mountains in Hebei province, China. *Ecol. Ind.* **129**, 967. <https://doi.org/10.1016/j.ecolind.2021.107967> (2021).
- Zhu, P., Huang, L., Xiao, T. & Wang, J. Dynamic changes of habitats in china's typical National nature reserves on Spatial and Temporal scales. *J. Geog. Sci.* **28**, 778–790. <https://doi.org/10.1007/s11442-018-1504-y> (2018).
- Zhang, X., Wan, W., Fan, H., Dong, X. & Lv, T. J. F. N. C. Temporal and Spatial responses of landscape patterns to habitat quality C.anges in the Poyang lake region, China. *J. Nat. Conserv.* **77**, 126546 (2024).
- Sherrouse, B. C., Semmens, D. J. & Clement, J. M. An application of social values for ecosystem services (SolVES) to three National forests in Colorado and Wyoming. *Ecol. Ind.* **36**, 68–79. <https://doi.org/10.1016/j.ecolind.2013.07.008> (2014).
- Lewis, N. S., Fox, E. W. & DeWitt, T. H. Estimating the distribution of harvested estuarine bivalves with natural-history-based habitat suitability models. *Estuar. Coastal. Shelf Sci.* **219**, 453–472. <https://doi.org/10.1016/j.ecss.2019.02.009> (2019).
- Terrado, M. et al. Model development for the assessment of terrestrial and aquatic habitat quality in conservation planning. *Sci. Total Environ.* **540**, 63–70. <https://doi.org/10.1016/j.scitotenv.2015.03.064> (2016).
- Zhao, B., Li, S. & Liu, Z. Multi-scenario simulation and prediction of regional habitat quality based on a system dynamic and patch-generating land-use simulation coupling model—A case study of Jilin Province. *Sustainability* **14**, 303. <https://doi.org/10.3390/su14095303> (2022).
- Chen, S. & Liu, X. Spatio-temporal variations of habitat quality and its driving factors in the Yangtze river Delta region of China. *Global Ecol. Conserv.* **52**, 978. <https://doi.org/10.1016/j.gecco.2024.e02978> (2024).
- Wu, L., Sun, C. & Fan, F. Estimating the characteristic Spatiotemporal variation in habitat quality using the invest Model—A case study from Guangdong-Hong Kong-Macao greater Bay area. *Remote Sens.* **13**, 8. <https://doi.org/10.3390/rs13051008> (2021).
- Janus, J. & Bozek, P. Land abandonment in Poland after the collapse of socialism: over a quarter of a century of increasing tree cover on agricultural land. *Ecol. Eng.* **138**, 106–117. <https://doi.org/10.1016/j.ecoleng.2019.06.017> (2019).

24. Wu, J., Hou, Y. & Cui, Z. Coupled InVEST–MGWR modeling to analyze the impacts of changing landscape patterns on habitat quality in the Fen river basin. *Sci. Rep.* **14**, 1 (2024).
25. Qamer, F. M. et al. Mapping deforestation and forest degradation patterns in Western Himalaya, Pakistan. *Remote Sens.* **8**, 385. <https://doi.org/10.3390/rs8050385> (2016).
26. Li, M. et al. Evolution of habitat quality and its topographic gradient effect in Northwest Hubei Province from 2000 to 2020 based on the invest model. *Land* **10**, 857. <https://doi.org/10.3390/land10080857> (2021).
27. Tang, F. et al. Spatio-temporal variation and coupling coordination relationship between urbanisation and habitat quality in the Grand Canal, China. *Land Use Policy*. **117**, 119. <https://doi.org/10.1016/j.landusepol.2022.106119> (2022).
28. Wang, Y. et al. Characterization and multi-scenario prediction of habitat quality evolution in the Bosten Lake watershed based on the invest and PLUS models. *Sustainability* **16**, 202. <https://doi.org/10.3390/su16104202> (2024).
29. Hongying, C., Ziwei, W., Xiaoyong, L., You, L. & Yongbing, Z. Research on the regional environmental impact and risk assessment affected by mineral resource development: A case study of the Taojia River watershed in Hunan. *Front. Ecol. Evol.* **10**, 1 (2022).
30. Bohan, W. et al. Effects of environmental factors on soil bacterial community structure and diversity in different contaminated districts of Southwest China mine tailings. *Sci. Total Environ.* **802**, 149899–149899 (2022).
31. Zhang, T. L. et al. Spatial distribution, speciation, and ecological risk assessment of heavy metals in surface sediments of Dongjiang Lake, Hunan Province. *Huanjing Kexue*. **44**, 4896–4905. <https://doi.org/10.13227/j.hj.kx.202209060> (2023).
32. Li, Z., Zheng, K. & Zhong, Q. Comprehensive evaluation and spatio-temporal pattern of green development in Hunan Province, China. *Sustainability* **14**, 19. <https://doi.org/10.3390/su14116819> (2022).
33. Peng, X. L. *Studies on the Integrative Development of Hunan Use Mineral Resources and Eco-environment* (2011).
34. Xiong, Q., Hong, Q. & Chen, W. Temporal and Spatial response of ecological environmental quality to land use transfer in Nanling Mountain region, China based on RSEI: A case study of Longnan City. *Land* **13**, 675. <https://doi.org/10.3390/land13050675> (2024).
35. Yang, L., Shi, L., Li, J. & Kong, H. Spatio-temporal pattern change of LULC and its response to climate in the loess plateau, China. *Sci. Rep.* **14**, 1. <https://doi.org/10.1038/s41598-024-73945-0> (2024).
36. Wang, Y., Xia, T., Shataer, R., Zhang, S. & Li, Z. Analysis of characteristics and driving factors of land-use changes in the Tarim River basin from 1990 to 2018. *Sustainability* **13**, 263. <https://doi.org/10.3390/su131810263> (2021).
37. Gao, X. et al. Spatio-temporal distribution and transformation of cropland in geomorphologic regions of China during 1990–2015. *J. Geog. Sci.* **29**, 180–196. <https://doi.org/10.1007/s11442-019-1591-4> (2019).
38. Chen, P., Duan, J. & Wang, Y. Spatio-temporal evolution and driving forces of urban gravity centers and ecological security risk gravity centers in China. *Ecol. Ind.* **170**, 25. <https://doi.org/10.1016/j.ecolind.2024.113025> (2025).
39. Zheng, G. et al. Spatio-temporal evolution analysis of landscape pattern and habitat quality in the Qinghai Province section of the Yellow River basin from 2000 to 2022 based on invest model. *J. Arid Land*. **16**, 1183–1196. <https://doi.org/10.1007/s40333-024-0107-y> (2024).
40. Wu, J., Hou, Y. & Cui, Z. Coupled InVEST–MGWR modeling to analyze the impacts of changing landscape patterns on habitat quality in the Fen River basin. *Sci. Rep.* **14**, 9. <https://doi.org/10.1038/s41598-024-64012-9> (2024).
41. Yang, F., Yang, L., Fang, Q. & Yao, X. Impact of landscape pattern on habitat quality in the Yangtze River Economic Belt from 2000 to 2030. *Ecol. Ind.* **166**, 480. <https://doi.org/10.1016/j.ecolind.2024.112480> (2024).
42. Zhao, G., Hoermann, G., Fohrer, N., Zhang, Z. & Zhai, J. Streamflow trends and climate variability impacts in Poyang Lake basin, China. *Water Resour. Manage.* **24**, 689–706. <https://doi.org/10.1007/s11269-009-9465-7> (2010).
43. Liu, Y., Li, Y., Li, S. & Motesharrei, S. Spatial and Temporal patterns of global NDVI trends: correlations with climate and human factors. *Remote Sens.* **7**, 13233–13250. <https://doi.org/10.3390/rs71013233> (2015).
44. Ban, Y. et al. Effect of urbanization on aerosol optical depth over Beijing: land use and surface temperature analysis. *Urban Clim.* **51**, 655. <https://doi.org/10.1016/j.uclim.2023.101655> (2023).
45. Wang, W., Wen, Y., Chen, W. & Qu, Y. Spatial-temporal coupling coordination relationship between urban green infrastructure construction and economic development in China. *Land* **13**, 95. <https://doi.org/10.3390/land13071095> (2024).
46. Liao, C. et al. Influencing factors, and development paths of rural tourism resources in Guangdong Province. *Land* **11**. <https://doi.org/10.3390/land11112046> (2022).
47. Liang, X. et al. Understanding the drivers of sustainable land expansion using a patch-generating land use simulation (PLUS) model: A case study in Wuhan, China. *Computers Environ. Urban Syst.* **85**, 69. <https://doi.org/10.1016/j.compenvurbysys.2020.101569> (2021).
48. Xu, L. et al. Forecasting urban land use change based on cellular automata and the PLUS model. *Land* **11**, 52. <https://doi.org/10.3390/land11050652> (2022).
49. Xu, X., Yu, J. & Wang, F. Analysis of ecosystem service drivers based on interpretive machine learning: a case study of Zhejiang Province, China. *Environ. Sci. Pollut. Res.* **29**, 64060–64076. <https://doi.org/10.1007/s11356-022-20311-0> (2022).
50. Cao, S. et al. Understanding spatial–temporal interactions of ecosystem services and their drivers in a multi-scale perspective of Miluo using multi-source remote sensing data. *Remote Sens.* **15**, 479. <https://doi.org/10.3390/rs15143479> (2023).
51. Huang, J. et al. Spatial and Temporal characterization of critical ecosystem services in China's terrestrial area, 2000–2020: trade-off synergies, driving mechanisms and functional zoning. *Front. Ecol. Evol.* **12**, 683. <https://doi.org/10.3389/fevo.2024.1443683> (2024).
52. Chen, S., Liu, X., Yang, L. & Zhu, Z. Variations in ecosystem service value and its driving factors in the Nanjing metropolitan area of China. *Forests* **14**, 113. <https://doi.org/10.3390/f14010113> (2023).
53. Chen, J. et al. Spatial and Temporal heterogeneity analysis of water conservation in Beijing–Tianjin–Hebei urban agglomeration based on the geodetector and Spatial elastic coefficient trajectory models. *Geohealth* **4**, 248. <https://doi.org/10.1029/2020gh000248> (2020).
54. Li, X. et al. Precipitation and soil texture dominate the Spatiotemporal changes in the carbon–water coupling coordination in Taihang Mountains, China. *J. Geog. Sci.* **35**, 521–551. <https://doi.org/10.1007/s11442-025-2333-4> (2025).
55. Li, W. et al. Spatial and Temporal evolution patterns of habitat quality under tea plantation expansion and multi-scenario simulation study: Anxi County as an example. *Land* **12**, 1308 (2023).
56. Liu, Y., Huang, X. & Liu, Y. Detection of long-term land use and ecosystem services dynamics in the loess Hilly–Gully region based on artificial intelligence and multiple models. *J. Clean. Prod.* **447**, 141560. <https://doi.org/10.1016/j.jclepro.2024.141560> (2024).
57. Briner, S., Elkin, C. & Huber, R. Grêt-Regamey, A. Assessing the impacts of economic and climate changes on land-use in mountain regions: A Spatial dynamic modeling approach. *Agric. Ecosyst. Environ.* **149**, 50–63. <https://doi.org/10.1016/j.agee.2011.12.011> (2012).
58. Zhu, Z., Mei, Z., Li, S., Ren, G. & Feng, Y. Evaluation of ecological carrying capacity and identification of its influencing factors based on remote sensing and geographic information system: a case study of the Yellow River basin in Shaanxi. *Land* **11**, 80. <https://doi.org/10.3390/land11071080> (2022).
59. Liu, Y., Zuo, R. & Dong, Y. Analysis of Temporal and Spatial characteristics of urban expansion in Xiaonan district from 1990 to 2020 using time series Landsat imagery. *Remote Sens.* **13**, 99. <https://doi.org/10.3390/rs13214299> (2021).
60. Wang, D., Hao, H., Liu, H., Sun, L. & Li, Y. Spatial–temporal changes of landscape and habitat quality in typical ecologically fragile areas of Western China over the past 40 years: A case study of the Ningxia Hui autonomous region. *Ecol. Evol.* **14**, 47. <https://doi.org/10.1002/ece3.10847> (2024).
61. Hu, L. et al. Impacts of land-use change on the habitat suitability and connectivity of giant panda. *Global Ecol. Conserv.* **53**, e03019. <https://doi.org/10.1016/j.gecco.2024.e03019> (2024).

62. Lv, Z. et al. Prioritizing green spaces for biodiversity conservation in Beijing based on habitat network connectivity. *Sustainability* **11**, 42. <https://doi.org/10.3390/su11072042> (2019).
63. Zhang, X., Qin, X., Alvarez, F., Chen, Z. & Wu, Z. Potential impact of land-use change on habitat quality in the distribution range of crocodile lizards in China. *Ecol. Evol.* **12**, e9390. <https://doi.org/10.1002/ece3.9390> (2022).
64. Sontter, L. J. et al. Conservation implications and opportunities of mining activities for terrestrial mammal habitat. *Conserv. Sci. Pract.* **4**, e12806. <https://doi.org/10.1111/csp2.12806> (2022).
65. Gontier, M. Scale issues in the assessment of ecological impacts using a GIS-based habitat model—A case study for the Stockholm region. *Environ. Impact Assess. Rev.* **27**, 440–459. <https://doi.org/10.1016/j.eiar.2007.02.003> (2007).
66. Wang, B., Oguchi, T. & Liang, X. Evaluating future habitat quality responding to land use change under different City compaction scenarios in Southern China. *Cities* **140**, 410. <https://doi.org/10.1016/j.cities.2023.104410> (2023).
67. Ahmadi Mirghaed, F. & Souri, B. Relationships between habitat quality and ecological properties across Ziarat basin in Northern Iran. *Environ. Dev. Sustain.* **23**, 16192–16207. <https://doi.org/10.1007/s10668-021-01343-x> (2021).
68. Michaud, J. S., Coops, N. C., Andrew, M. E. & Wulder, M. A. Characterising Spatiotemporal environmental and natural variation using a dynamic habitat index throughout the Province of Ontario. *Ecol. Ind.* **18**, 303–311. <https://doi.org/10.1016/j.ecolind.2011.11.027> (2012).
69. Yang, L. et al. Declining urban-rural population densities: how do they affect natural habitat? *Land. Degrad. Dev.* **36**, 1939–1951. <https://doi.org/10.1002/ldr.5473> (2025).
70. Liu, Y. et al. Habitat quality assessment and driving factors analysis of Guangdong province, China. *Sustainability* **15**, 15. <https://doi.org/10.3390/su151511615> (2023).
71. Xu, Y. et al. Spatial and Temporal analysis of habitat quality in the yellow river basin based on land-use transition and its driving forces. *Land* **14**, 59. <https://doi.org/10.3390/land14040759> (2025).
72. Jarsjo, J., Chalov, S. R., Pietron, J., Alekseenko, A. V. & Thorslund, J. Patterns of soil contamination, erosion and river loading of metals in a gold mining region of Northern Mongolia. *Reg. Environ. Chang.* **17**, 1991–2005. <https://doi.org/10.1007/s10113-017-1169-6> (2017).
73. Nordstrom, D. K. Hydrogeochemical processes governing the origin, transport and fate of major and trace elements from mine wastes and mineralized rock to surface waters. *Appl. Geochem.* **26**, 1777–1791. <https://doi.org/10.1016/j.apgeochem.2011.06.002> (2011).
74. Niningsih, L., Alikodra, H. S., Atmoko, S. S. U. & Mulyani, Y. A. Characteristic of orangutan habitat in coal mining rehabilitation area in East Kalimantan, Indonesia. *Manajemen Hutan Tropika.* **23**, 37–49. <https://doi.org/10.7226/jtfm.23.1.37> (2017).
75. Safaei, M. et al. Spatial scale effect of Sentinel-2, Landsat OLI, and MODIS imagery in the assessment of landscape condition of Zagros mountains. *Geocarto Int.* **37**, 5345–5362. <https://doi.org/10.1080/10106049.2021.1914745> (2022).

Author contributions

Y.S. and X.L. conceived the study and wrote the manuscript. Y.Y., H.W., and C.Z. organized and analyzed the data. Z.C., Z.D., and Y.L. revised the manuscript. All the authors reviewed the manuscript.

Funding

This research was funded by the China Postdoctoral Science Foundation, Grant Number 2024M761587; the Key Research and Development Program of Hunan Province, Grant Number 2024JK2025.

Declarations

Competing interests

The authors declare no competing interests.

Additional information

Supplementary Information The online version contains supplementary material available at <https://doi.org/10.1038/s41598-025-05369-3>.

Correspondence and requests for materials should be addressed to Y.L.

Reprints and permissions information is available at www.nature.com/reprints.

Publisher's note Springer Nature remains neutral with regard to jurisdictional claims in published maps and institutional affiliations.

Open Access This article is licensed under a Creative Commons Attribution-NonCommercial-NoDerivatives 4.0 International License, which permits any non-commercial use, sharing, distribution and reproduction in any medium or format, as long as you give appropriate credit to the original author(s) and the source, provide a link to the Creative Commons licence, and indicate if you modified the licensed material. You do not have permission under this licence to share adapted material derived from this article or parts of it. The images or other third party material in this article are included in the article's Creative Commons licence, unless indicated otherwise in a credit line to the material. If material is not included in the article's Creative Commons licence and your intended use is not permitted by statutory regulation or exceeds the permitted use, you will need to obtain permission directly from the copyright holder. To view a copy of this licence, visit <http://creativecommons.org/licenses/by-nc-nd/4.0/>.

© The Author(s) 2025